



university of
 groningen

faculty of mathematics
 and natural sciences

NANOSTRUCTURED MATERIALS AND INTERFACES

Crystallisation of GeSb films

using a heating plate and a laser

Floorke Koops
s1639633

Bachelor Thesis
22-01-2013

Mentor
G. Eising, MSc.

Supervisors
prof. dr. ir. B.J. Kooi
dr. G. Palazantsas

During this bachelor research the crystallisation of germanium antimony was investigated in two different ways. In the first experiments the samples were heated by a heating plate. The crystal growth in thin films of $\text{Ge}_7\text{Sb}_{93}$, $\text{Ge}_9\text{Sb}_{91}$ and $\text{Ge}_{10}\text{Sb}_{90}$ was explored. In $\text{Ge}_7\text{Sb}_{93}$ films the crystals grew approximately 50 per cent faster if the samples were preheated at 100 °C for 12 hours, compared to when they were directly heated to the final temperatures. In $\text{Ge}_9\text{Sb}_{91}$ films there are two types of crystals. At 180 °C only slow growing crystals form and at 188 °C only fast growing crystals arise. In between these temperatures both crystal types coexist. The crystals that grow in films of $\text{Ge}_{10}\text{Sb}_{90}$ are very small, so the measurement techniques are presumably not accurate enough to see a larger crystal growth rate in samples that are preheated. In the second experiments a sample of $\text{Ge}_{10}\text{Sb}_{90}$ was irradiated with a high power laser using short pulses. It is possible to crystallise a material with the built setup, but the crystallisation should still be optimised and a next study should tell if it is also possible to melt-quench a material with the high power laser.

Table of contents

1	Introduction	2
2	Theory.....	3
	2.1 Phase Change Materials	3
	2.2 Crystallisation	3
	2.3 Germanium Antimony.....	4
	2.4 Comatic aberration	4
3	Materials and Methods.....	5
	3.1 Heating Plate	5
	3.1.1 Setup.....	5
	3.1.2 Experiments.....	6
	3.2 Laser	7
	3.2.1 Setup 1	8
	3.2.2 Setup 2.....	10
	3.2.3 Setup 3.....	12
	3.2.4 Experiments.....	12
4	Results	14
	4.1 Heating Plate	14
	4.2 Laser	16
	4.2.1 Setup 3.....	17
	4.2.2 Setup 2.....	17
5	Discussion	20
	5.1 Heating Plate	20
	5.2 Laser	21
6	Conclusions	22
7	Special Thanks.....	23
8	References	24
	Appendix A.....	25
	Appendix B.....	26

1 Introduction

In the past decades digital information has become more important in all aspects of life. Because of the growing importance, a higher storage capacity on smaller data storage devices is desired and to accomplish this, a complete new research field has originated.

The possibilities to meet these desires is limited for the conventional methods using FLASH memory. Nevertheless, Phase Change Materials (PCM's) can cause a scientific breakthrough because they are known for their property to work as a storage device using the amorphous and crystalline state. The Nanostructured Materials and Interfaces group of the University of Groningen conducts research in this field.

This thesis describes the Bachelor research performed within the Nanostructured Materials and Interfaces group to contribute to their research. The aim was to see how crystals grow in germanium antimony (GeSb) using different methods. Hereby, building the setup was an important point of interest.

The first method used to analyse the crystal growth was heating the samples with a heating plate and measuring the growth rate with a high-speed camera. The second technique was to heat the sample with laser pulses of a certain power and duration. The laser setup was built and a method used to store and process the future results was programmed.

2 Theory

This chapter gives a short outline of PCM's, germanium antimony and crystallisation. In addition, it will briefly describe the phenomenon of comatic aberration.

2.1 Phase Change Materials

The discovery of PCM's started in the early 1900s with the work of Alan T. Waterman when he noticed a change in the conductivity of matter when it was heated. However, the real breakthrough came in the sixties of the last century when Stanford R. Ovshinsky revealed reversible switching in memory devices. The paper of Ovshinsky about this phenomenon still is the most cited with respect to PCM's. [1]

PCM's are materials that can switch in nanoseconds between an amorphous and a crystalline state [2]. In crystalline phase the atoms are long-range ordered, as shown on the left of Figure 1, and have three-dimensional repetitive patterns. By contrast, in amorphous phase the atoms are only short-range ordered, as shown on the right of Figure 1, and there is no three-dimensional repetitive pattern. [3]

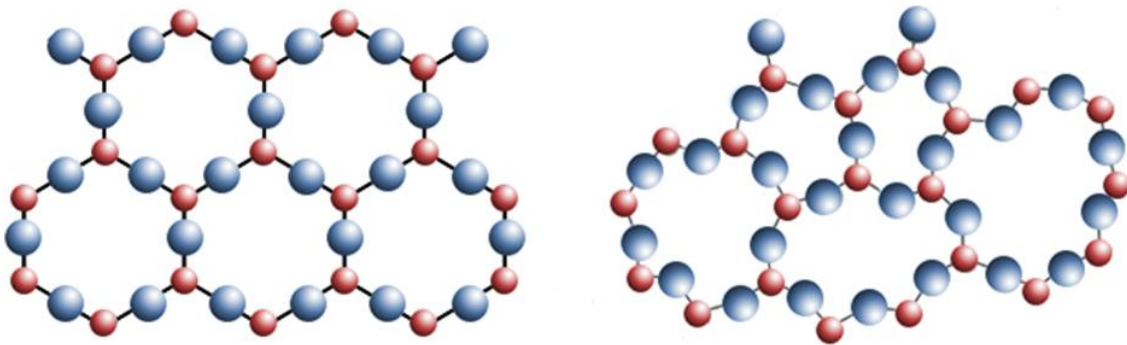


Figure 1. Schematic 2D illustration of crystalline (left) and amorphous (right) SiO₂. [4]

PCM's are widely used for everyday items, such as rewritable optical disks. This is largely because of their durability for many crystallisation and amorphisation cycles, which makes the items reliable. Also, minuscule volumes of the alloys can be crystallised and amorphised, which makes it possible to produce bits that are very small. [5]

2.2 Crystallisation

If a PCM is heated, it can change from the disordered, amorphous phase to the ordered, crystalline phase. This process is called crystallisation and consists of two parts. The first part is the initial formation of the crystals, which is named the crystal nucleation. The initial formation can start at an impurity, the so-called heterogeneous nucleation, or start in the interior of the material, the so-called homogeneous nucleation. In the second part of the process, called crystal growth, the formed crystals grow larger. [1]

The crystal growth rate can, in specific cases, be described by the Arrhenius equation $v = v_0 e^{E_a/kT}$ [6]. In this equation v_0 is the pre-exponential factor (e.g. in $\mu\text{m s}^{-1}$), E_a is the activation energy in eV or kJ/mol, k is the Boltzmann constant and T is the temperature in K. From this Arrhenius equation it can be seen that a plot of $\ln v$ versus $1/kT$ should give a linear relation. The slope of the line is then equal to the activation energy E_a and the intersection with the $\ln v$ axis gives the pre-exponential factor. [7]

After crystallisation, a sample can be amorphised again by heating the sample until it melts. After melting, the sample has to be cooled down very fast, so no crystals can originate and grow during quenching. This process is called melt-quenching.

2.3 Germanium Antimony

Germanium antimony (GeSb) is used in many different compositions, ranging from low Sb content to high Sb content. In this research only samples with high Sb content are used, which have been shown to be fast crystallising [8]. Thin films of GeSb with high Sb content crystallise and amorphise with laser pulses that have only nanoseconds of pulse duration [9].

2.4 Comatic aberration

Comatic aberration (coma) is caused by the laser being off-axis. With a monochromatic point source, for example a laser, the spot on the sample will be comet-like, which is shown in Figure 2. This is due to the fact that in every zone the sample is focussed at a different height, producing spots of increasing size. [10] The small spot at the vertex of the cone is the brightest and the largest spot has the lowest brightness. If the vertex points towards the optical axis, the comatic aberration is called negative and if the vertex points away from the optical axis, it is called positive comatic aberration. [11]

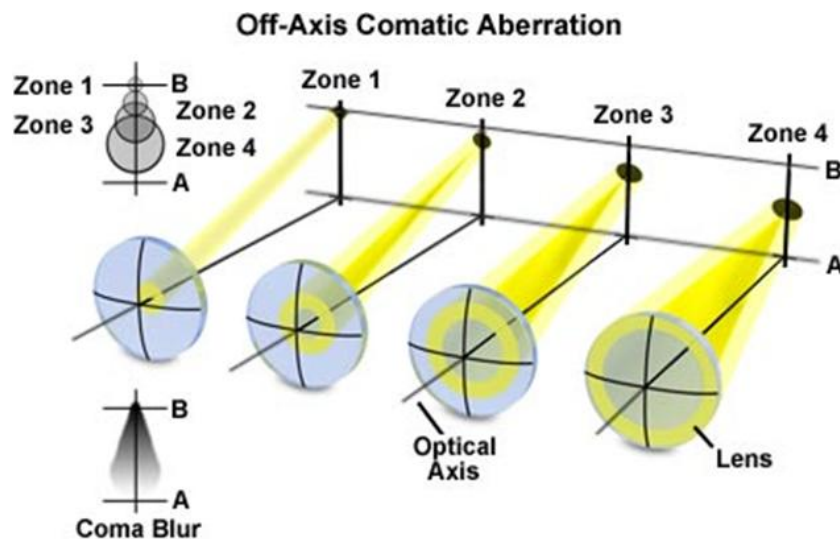


Figure 2. Illustration of positive comatic aberration. The rays passing through the periphery of the lens cause a large spot close to the optical axis and the rays passing through the centre of the lens cause a small spot further away from the optical axis. [10]

3 Materials and Methods

For the two types of experiments done with GeSb films different methods were used to examine the crystal growth. They will be discussed below.

3.1 Heating Plate

3.1.1 Setup

The setup for the experiments with the heating plate is displayed in Figure 3.

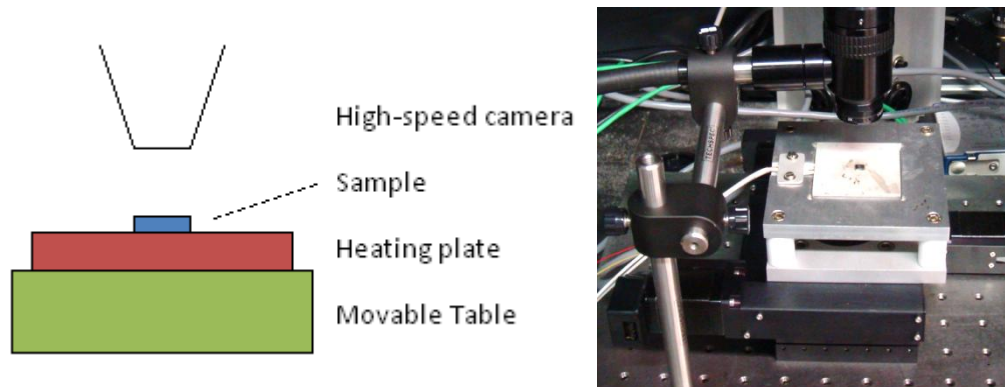


Figure 3. Schematic illustration (left) and image (right) of the setup of the experiments with the heating plate. Both show a movable table, a heating plate, a sample and a high-speed camera.

At the bottom a movable table is shown. With the software on the computer it is possible to move this table horizontally. It may be used to place the sample in the centre of the image of the high-speed camera, if placing it there manually is not satisfactory. It consists of three parts, two parts can be moved left and right and one part can be moved back and forth.

On top of the movable table is a heating plate. To control the temperature of this plate, a temperature control software script is written in Explosive, which is displayed in the program as shown in Table 1. With this control software it is possible to choose the temperature setpoint [°C], the slope of heating [°C/min] and the delay afterwards [s]. The delay afterwards is defined as the time it has to stay at the temperature setpoint after reaching it. If you put another temperature setpoint in the next row, this will become the new setpoint after the delay afterwards is expired; if you do not, the heater will turn off and the temperature will go back to room temperature. When no value is entered for the delay afterwards, the temperature will stay at the setpoint until you turn the heater off manually.

Temperature setpoint [°C]	Slope of heating [°C/min]	Delay afterwards [s]
100	20	600
140	20	

Table 1. Example of the software to control the temperature of the heating plate. In this case the temperature would rise with 20 °C per minute until it reaches 100 °C. After being 100 °C for 10 minutes, the temperature will rise to 140 °C, again with 20 °C per minute, where it will stay until the software is switched off.

A sample can be put on top of the heating plate. With the high-speed camera an image is obtained, which is also displayed with Explosive. These images can be saved on the computer automatically by choosing a map where they must be stored and setting how many seconds must elapse for the computer to record a new image.

3.1.2 Experiments

In this experiment the images obtained with the high-speed camera were analysed with Matlab using an already existing script written by G. Eising. The growth rate of crystals in a coating of 200 nm thick $\text{Ge}_7\text{Sb}_{93}$ on glass was examined at certain temperatures. The first set of samples was directly heated to temperatures ranging from 100 °C to 140 °C at a rate of 20 °C per minute. The second set was preheated at 100 °C for 12 hours, whereafter the sample was cooled down to room temperature again. Later the sample was heated to temperatures varying from 110 °C to 140 °C at a rate of 20 °C per minute. The aim was to see if there are differences in growth rate between these two groups.

Another experiment was done with 200 nm thick $\text{Ge}_{10}\text{Sb}_{90}$ on glass. The aim was to see if it was possible to analyse the crystals that would grow in this material in the same way as with films of $\text{Ge}_7\text{Sb}_{93}$. The crystals in $\text{Ge}_{10}\text{Sb}_{90}$ films are much smaller and it was not clear if the Matlab script is as well sufficient for these small crystals. To verify this, the analysis of the crystals was first done with Matlab and subsequently by hand. For the examination by hand the radius of the crystals of two images, that were taken at widely separated times, was estimated in pixels as shown in Figure 4. On the basis of these radii the growth rate was calculated.

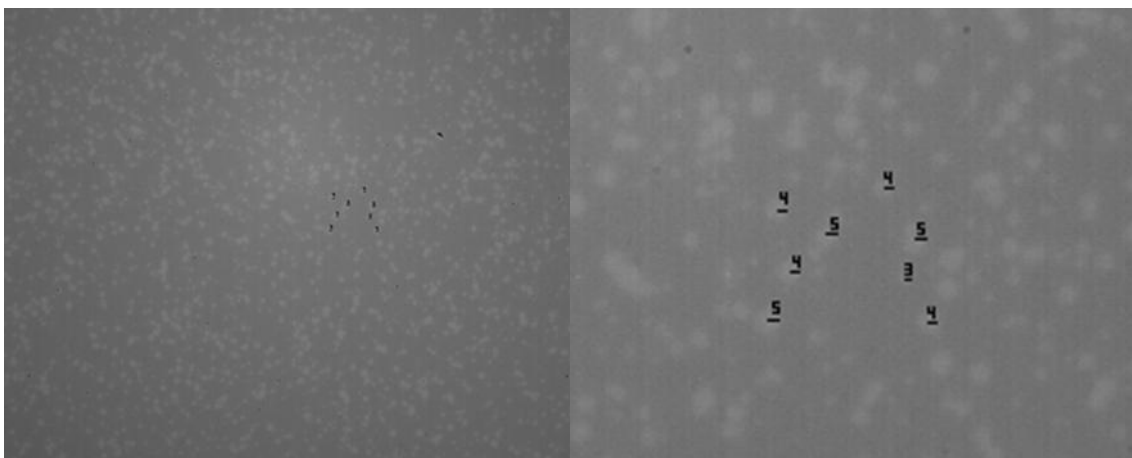


Figure 4. Illustration of the manual determination of the crystal size in partially crystallised 200 nm thick $\text{Ge}_{10}\text{Sb}_{90}$ on glass. The crystal size was examined by measuring the radius of the crystals in pixels, indicated with numbers. On the left is an overview and on the right a close-up.

The last experiment done with the high-speed camera was with 200nm thick $\text{Ge}_9\text{Sb}_{91}$ on glass. G. Eising did experiments with this material before and one of his results is shown in Figure 5. It shows that there are two types of crystals in films of $\text{Ge}_9\text{Sb}_{91}$ when it is heated at 185 °C: slow growing (small) crystals and fast growing (large) crystals. From his results he expected a dissimilar behaviour of the matter at 180 °C and 188 °C, at 180 °C it was expected to have only slow growing crystals and at 188 °C only fast growing crystals. This hypothesis was tested.

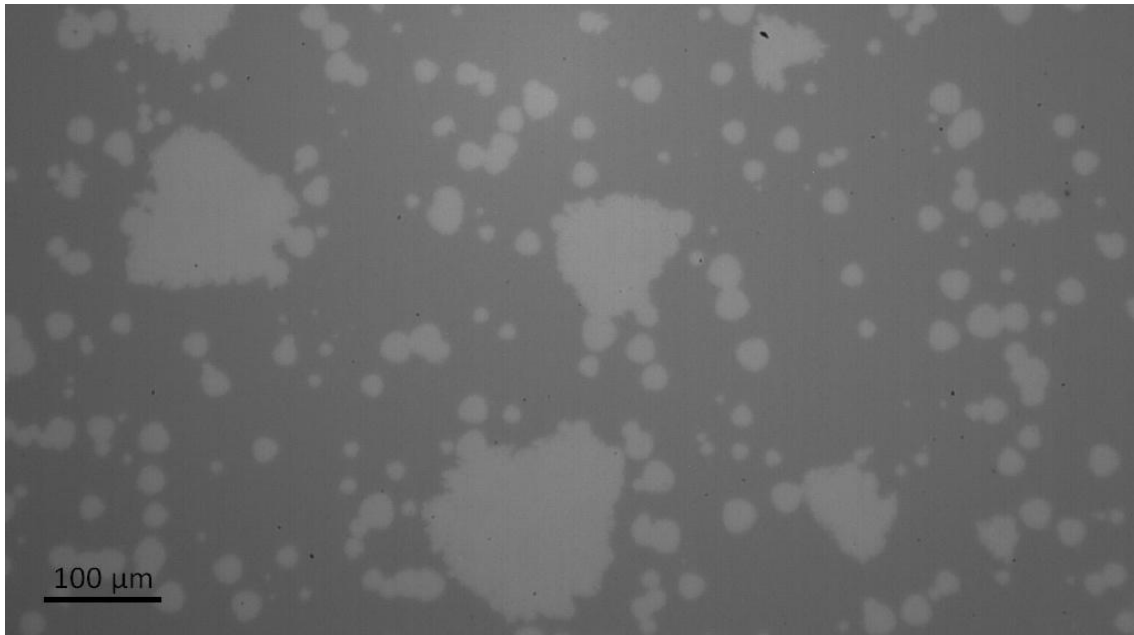


Figure 5. This image shows partially crystallised 200 nm thick $\text{Ge}_9\text{Sb}_{91}$ on glass. The sample was heated at 185 °C. Both the small growing crystals (small) and fast growing crystals (large) appear.

3.2 Laser

For the experiments with the laser, the setup had to be designed and built. Figure 6, Figure 8 and Figure 11 display the three setups that were considered during this research. In all figures the same indices are used for the constituent parts of the setup; these indices are shown in Table 2. In this chapter it will be widely discussed why they were considered at first and why two of them did eventually not make it.

A	Aspheric lens
B	Turning mirror
C	Dichroic beam splitter
D	50/50 beam splitter
E	Detector
F	Low power laser
G	Beam expander
H	High power laser

Table 2. An overview of the letters that appear in the schematic representations of the three setups that were considered during this research. Every letter corresponds to a certain component of the setup, which is shown next to the letter.

In all setups, like in the first experiment, the sample is placed on top of the heating plate, which is on a movable table. The sample is irradiated with the help of a collimating aspheric lens with a focal length of 3.1 mm. Because it is easier to build the setup horizontally instead of vertically, a turning mirror is placed above the lens at an angle of 45 degrees. To crystallise the sample it is irradiated with a high power laser. This laser was already bought and it has a wavelength of 643 nm and a diameter of 1 mm. The power of this laser is adjustable from 0.2 mW to 100 mW, but when used as a high power laser it has a power of 100 mW. For crystallisation with the high power laser, the sample must be focussed. This focusing is done by measuring the intensity of the reflection of the low power laser with a detector. After irradiation with the high power laser the intensity will be measured once more and the difference in intensity before and after will be used as a measure for crystal growth. The low power laser should have a power of less than 1 mW, because otherwise it can change the material.

3.2.1 Setup 1

The setup that was thought of first is displayed in Figure 6. The high power laser shines on a beam expander, which makes the diameter of the laser beam 5 mm. The beam goes through a dichroic beam splitter - which transmits light with a wavelength of 643 nm and reflects light with the wavelength of the low power laser - and irradiates the sample via the turning mirror and the lens.

The low power laser is placed above the beam expander. The beam goes through the 50/50 beam splitter, which transmits fifty per cent and reflects fifty per cent of it. The transmitted light is stopped and the reflected light passes on to the dichroic beam splitter. The wavelength of the low power laser must be chosen in such a way that the beam is reflected by the dichroic beam splitter. After reflection the beam goes further to the turning mirror and falls through the lens on the sample. The sample reflects the incoming light and the beam will go back the same way until the 50/50 beam splitter is reached. There it is reflected and transmitted for both 50 per cent. The transmitted light will fall on a detector, which measures the intensity of the returned light. The reflected light will go back into the laser, which is not that good for the laser, but there was no other option.

The difficulty of this setup was finding a dichroic beam splitter that transmits light of a wavelength of 643 nm and finding a low power laser that has the wavelength congruent with the reflection wavelength of the dichroic beam splitter.

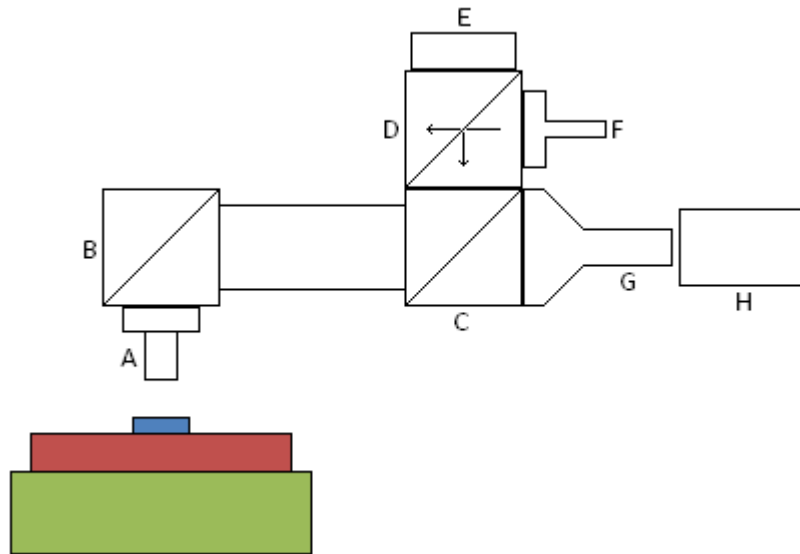


Figure 6. A schematic lateral view of the laser setup that was considered first. An explanation of the letters is shown in Table 2.

A dichroic beam splitter that transmits light with a wavelength of 643 nm was found at www.thorlabs.com. Figure 7 shows that this beam splitter transmits light with a wavelength between 620 and 700 nm and reflects light with a wavelength between 470 and 590 nm. Another comparable beam splitter was found at www.edmundoptics.com. This beam splitter transmits light with a wavelength between 633 and 700 nm and reflects light with a wavelength between 561 and 594 nm.

Thus, using one of these beam splitters, the low power laser must have a maximum wavelength of 594 nm. Such a laser was not found, so the setup had to be changed so that the high power laser beam is reflected and the low power laser beam is transmitted.

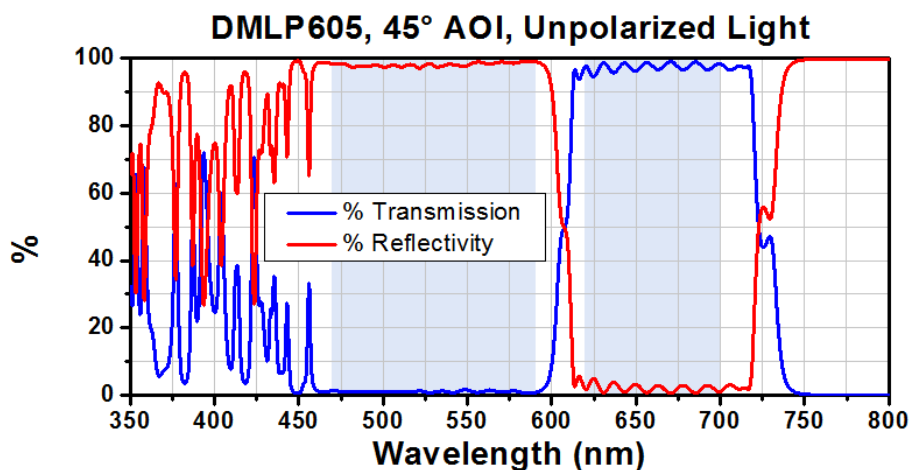


Figure 7. T/R plot of the beam splitter that was considered for setup 1. For wavelengths between 350 and 800 nm, the red line shows the percentage of reflectivity and the blue line shows the percentage of transmission.

The beam splitter transmits light with a wavelength between 620 and 700 nm and reflects light with a wavelength between 470 and 590 nm. [12]

3.2.2 Setup 2

A schematic top view of the setup that was thought of second is shown in Figure 8. Figure 10 shows the real setup. In this setup the high power laser again shines on a beam expander, which makes the diameter of the laser beam 5 mm. This time the beam is reflected by the dichroic beam splitter - which now reflects light with a wavelength of 643 nm and transmits light with the wavelength of the low power laser - whereafter it is reflected by the turning mirror and irradiates the sample through the lens.

The 50/50 beam splitter is attached on the right of the dichroic beam splitter. The low power laser shines on the 50/50 beam splitter, whereafter the 50 per cent beam reflection is stopped and the 50 per cent beam transmission passes on to the dichroic beam splitter. The wavelength of the low power laser must be chosen in such a way that the beam is transmitted by the dichroic beam splitter. After transmission by the dichroic beam splitter the beam falls on the sample via the turning mirror and the lens. The light is reflected by the sample and goes the same way back to the 50/50 beam splitter. After reflection it falls on the detector, which measures the intensity of the returned light. Also in this setup, like in setup 1, the transmitted beam will go back into the laser.

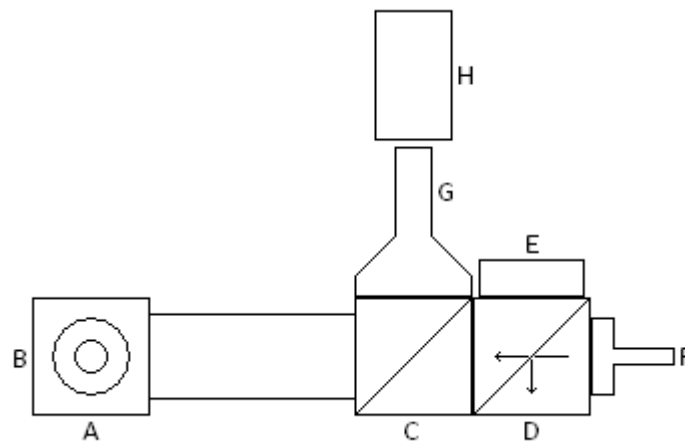


Figure 8. A schematic top view of the laser setup that was considered second. An explanation of the letters is shown in Table 2.

At www.thorlabs.com a dichroic beam splitter that reflects light with a wavelength of 643 nm was found. Because we want to focus the high power laser with the low power laser, it is best if the wavelengths of these lasers are as close as possible. Figure 9 shows that the beam splitter found transmits light with a wavelength of 400 to 872 nm and reflects light with a wavelength of 932 to 1300 nm. This means that the wavelengths of the lasers differ at least 289 nm, which is not ideal.

At www.edmundoptics.com another beam splitter was found. This one reflects light with a wavelength of 633 to 647 nm and transmits light with a wavelength of 671 to 790 nm. When this beam splitter is used, a low power laser of about 671 nm wavelength must be found. Then the wavelengths of the lasers differ only about 28 nm, which would be fine for the focusing.

3.2.3 Setup 3

Because the delivery time of the dichroic beam splitter was very long, a setup was built that uses only the laser of 643 nm, as shown in Figure 11. This laser is now used as both the high power laser and the low power laser. The laser shines on the beam expander, which makes the diameter of the beam 5 mm. The beam continues to the 50/50 beam splitter, which half reflects and half transmits it. The reflected part is stopped and the transmitted part goes to the sample through the turning mirror and the lens. At the sample it is reflected back to the 50/50 mirror. Half of the beam is transmitted back into the beam expander and half is reflected towards the detector.

At first the laser must be set to low power to focus the sample and to measure the intensity of the reflection, thereafter the laser must be set to high power to irradiate the sample and at last the laser must again be set to low power to measure the intensity after irradiation. The disadvantage of this setup is that, in contrast with setup 2, it is not possible to measure the intensity and irradiate the sample at the same time.

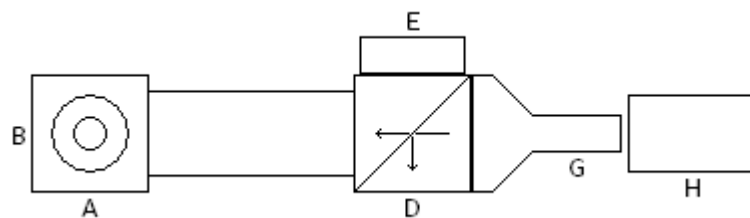


Figure 11. A schematic top view of the laser setup that was considered third. This setup uses only one laser. An explanation of the letters is shown in Table 2.

3.2.4 Experiments

The ultimate aim of the experiments is to repetitive crystallise and melt-quench $\text{Ge}_{10}\text{Sb}_{90}$ films with high power laser pulses. To achieve that, some pulse durations must be tried for a couple of powers and a diagram like Figure 12 should give an optimum. However, for now the aim of the experiments was to see if it was possible to crystallise $\text{Ge}_{10}\text{Sb}_{90}$ films with high power laser pulses at all. First, a sample of $\text{Ge}_{10}\text{Sb}_{90}$ was brought in focus manually. As described earlier in this chapter, the detector measured the intensity of the reflected beam of the low power laser. This intensity was measured as a current using a Keithley Digital Multimeter.

When the sample is in focus, which is when the intensity has its maximum value, a program written by G. Eising can be run. In this program it is possible to choose the range of duration and power of the high power laser pulse and the distance that the sample must be moved between two pulses. Once activated, it will repeatedly irradiate the sample until all the given powers and the given durations have been applied. During the irradiation, the following parameters are automatically saved in a text file, as shown in Table 3: 1) the measurement number 2) the relative x-value, starting with 0 for the most left measurement and adding 1 for every step to the right 3) the relative y-value, starting with 0 for the lowest measurement and adding 1 for every step upwards 4) the pulse duration in nanoseconds 5) the power of the pulse in milliwatt 6) the intensity of the reflected beam before irradiation with the high power laser 7) the intensity of the reflected beam after irradiation with the high power laser.

Measurement	x-value	y-value	Pulse duration (ns)	Power (mW)	Intensity before irradiation (nA)	Intensity after irradiation (nA)
1	0	0	10	10	60	60
2	0	1	10	20	60	61
3	1	0	20	10	60	62
4	1	1	20	20	60	64

Table 3. Example of the way the data is saved in a text file by the program that can be used to examine the crystal growth.

The saved text file can be analysed using the Matlab script shown in Appendix B. This script makes a diagram of the intensity differences measured at the diverse powers and pulse durations, as shown in Figure 12. On the x-axis the pulse durations are shown and on the y-axis the power is presented. Every combination of pulse duration and power will correspond with a box; if the box is blue it means that the intensity after irradiation was not much higher than the intensity before irradiation, a red box means that the intensity changed a lot by irradiation.

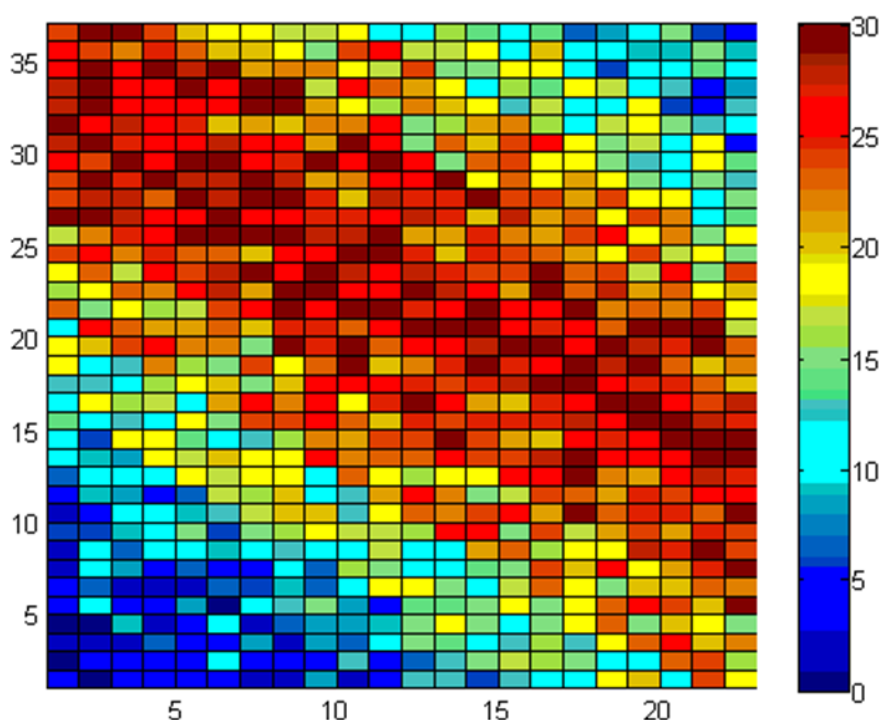


Figure 12. Example of the intensity matrix produced by the Matlab script. The x-axis contains the values of the pulse durations (e.g. in ns) and the y-axis the values of the power of the high power laser in mW. The scale on the right displays the change in intensity (e.g. in nA). Every couple of power and pulse duration corresponds to a box and the colour of that box displays the change in the intensity of the reflected beam.

For the measurements in this bachelor research the program of G. Eising was not used, but they were all done by hand. After focusing, the high power laser was set to Digital - the laser can be controlled digitally with pulses - to make spots and set to CW - the laser gives a continuous wave - to make stripes. The measurements done were used to improve the setup and to see what the possibilities of crystallisation are.

4 Results

4.1 Heating Plate

As described in section 3.1.2 the crystal growth rate in $\text{Ge}_7\text{Sb}_{93}$ films was examined as a function of the temperature. If the Arrhenius equation mentioned in section 2.3 holds, there exists a linear relation between the logarithm of the crystal growth rate and the reciprocal temperature. Therefore in Figure 13 the trend line through the plotted points should be linear. The circles in Figure 13 show the outcomes of the samples that were directly heated to the final temperature. The squares in Figure 13 show the outcomes of the second set of samples, which were preheated at 100 °C and thereafter heated to the final temperature. The red circle at 100 °C and the red square at 110 °C will be discussed in Chapter 5.

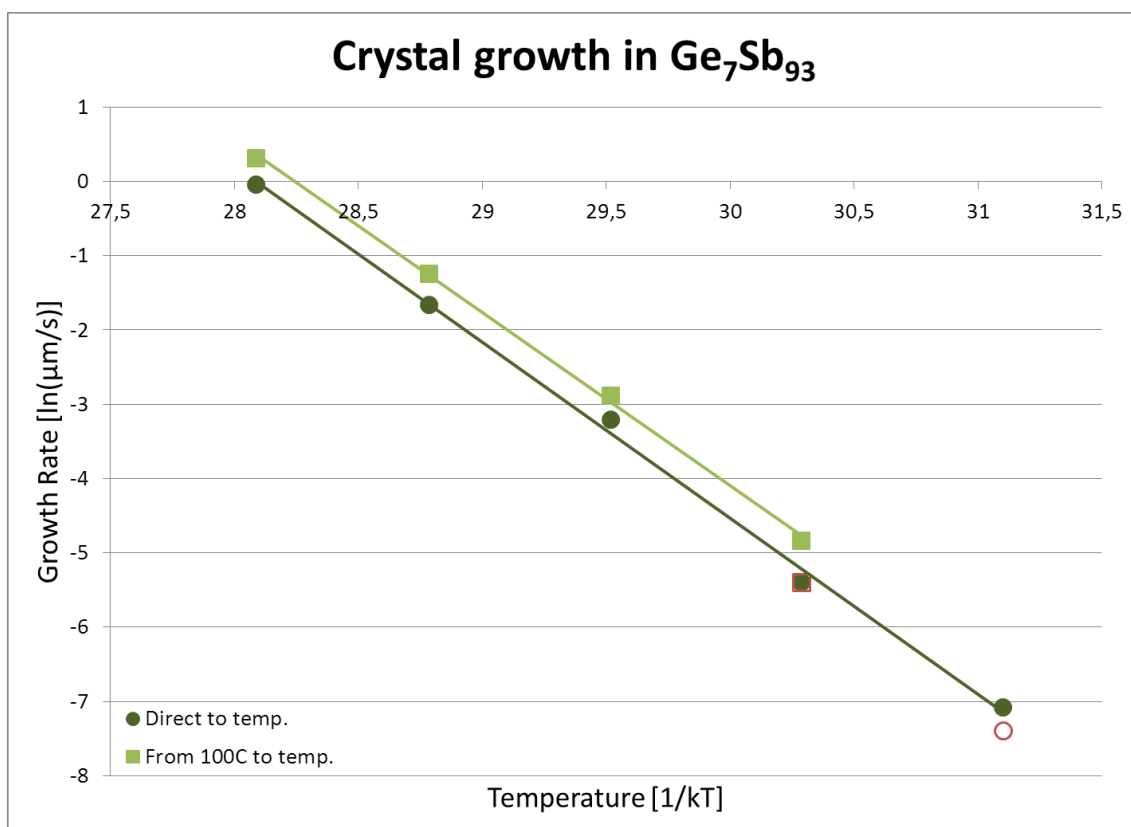


Figure 13. This graph shows the crystal growth rate in $\text{Ge}_7\text{Sb}_{93}$ films against the reciprocal temperature. The squares show the result of the samples that were preheated and the squares show the results of the samples that were not preheated. In the preheated samples the crystals grow faster than in the non-preheated samples.

The crystals of the samples that were directly heated to the final temperature have a lower growth rate than those that were preheated for 12 hours at 100 °C. In the samples that were preheated the crystals grew about 50 per cent faster than the crystals in the directly heated samples, varying from 38 per cent to 75 per cent faster. Preheating of a sample thus has a positive influence on the growth rate of the crystals in that sample.

A small difference was found in the activation energy of growth for those two groups by analysing the slope of the trend lines. In the directly heated group an activation energy of $E_a = 2.37$ eV was found and in the preheated group an activation energy of $E_a = 2.33$ eV was found. As can be seen in Figure 13, the points of the non-preheated samples deviate substantially from the trend line. Therefore, if one of these measured values was slightly different, the trend lines might as well have the exact same slope and thus both groups could have the same activation energy.

The growth rates of the crystals in $\text{Ge}_{10}\text{Sb}_{90}$ films are again logarithmically plotted against the reciprocal temperature in Figure 14. The diamonds show the outcomes of the crystal growth rate that was analysed with Matlab and the triangles show the results of the manual calculation of the crystal growth rate. To give an idea of the scale, the results of the experiments with $\text{Ge}_7\text{Sb}_{93}$ films are also shown as the red squares and circles on the right.

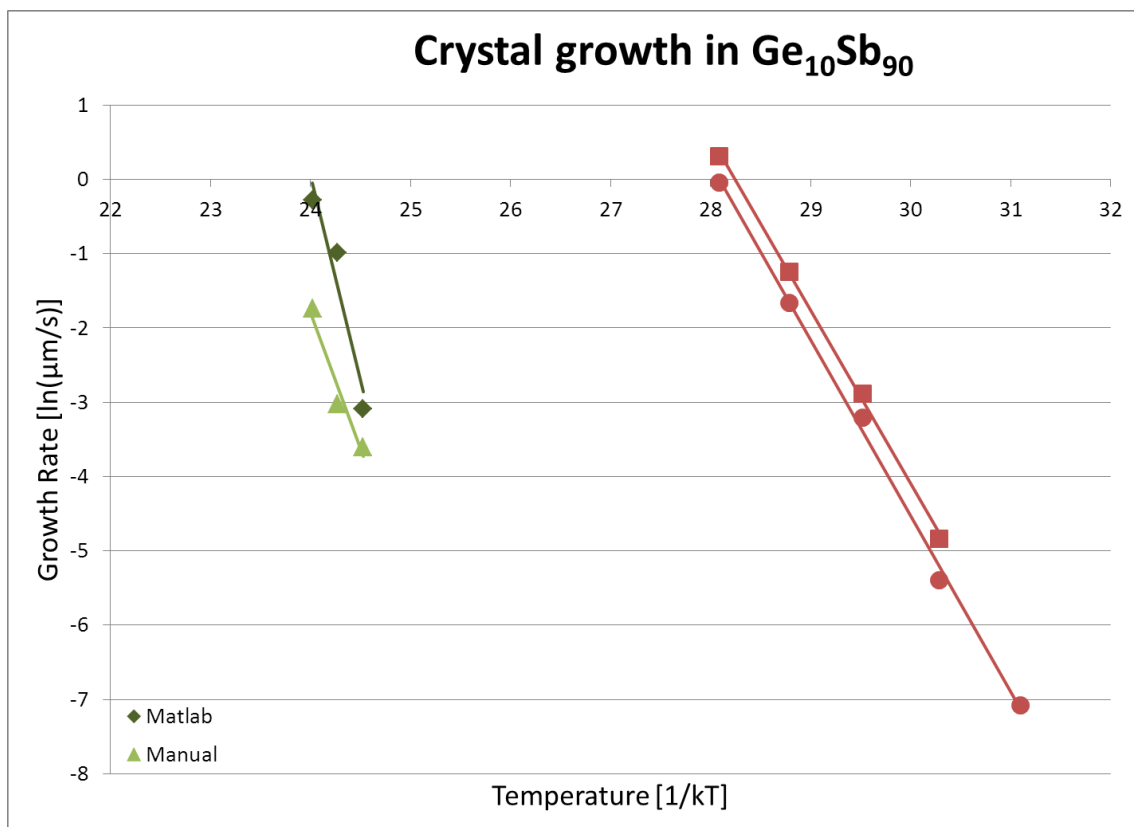


Figure 14. This graph shows in green the crystal growth rate in $\text{Ge}_{10}\text{Sb}_{90}$ films against the reciprocal temperature. The results of Matlab are displayed as diamonds and the manual results are displayed as triangles. The red squares and circles are the results with $\text{Ge}_7\text{Sb}_{93}$, that are also shown in Figure 13.

The manual calculated growth rate is close to the growth rate obtained with Matlab; the outcomes of the analysis with Matlab are of the right magnitude. Nevertheless, it seems as if the calculations with Matlab are not accurate enough to see the same difference in films of $\text{Ge}_{10}\text{Sb}_{90}$ as in $\text{Ge}_7\text{Sb}_{93}$ films; a difference in crystal growth rate between samples that are preheated and samples that are not.

As described in section 3.1.2 it is expected that when a sample of $\text{Ge}_9\text{Sb}_{91}$ is heated at a temperature of 180°C only slow crystals will grow and when a sample of the same material is heated at a temperature of 188°C only fast crystals will grow. Figure 15 shows two images of crystal growth in films of $\text{Ge}_9\text{Sb}_{91}$. Both images have the same scale of 1060 pixels per millimetre. In the sample that was heated at a temperature of 180°C the crystals grew after half an hour and in the sample that was heated at a temperature of 188°C the crystals grew after 15 seconds. At a temperature of 180°C only the crystals with a low growth rate appeared, as shown on the left of Figure 15, and at a temperature of 188°C only the crystals with a high growth rate were present, as shown on the right of Figure 15. These results indicate that the hypothesis stated in section 3.1.2 is correct.

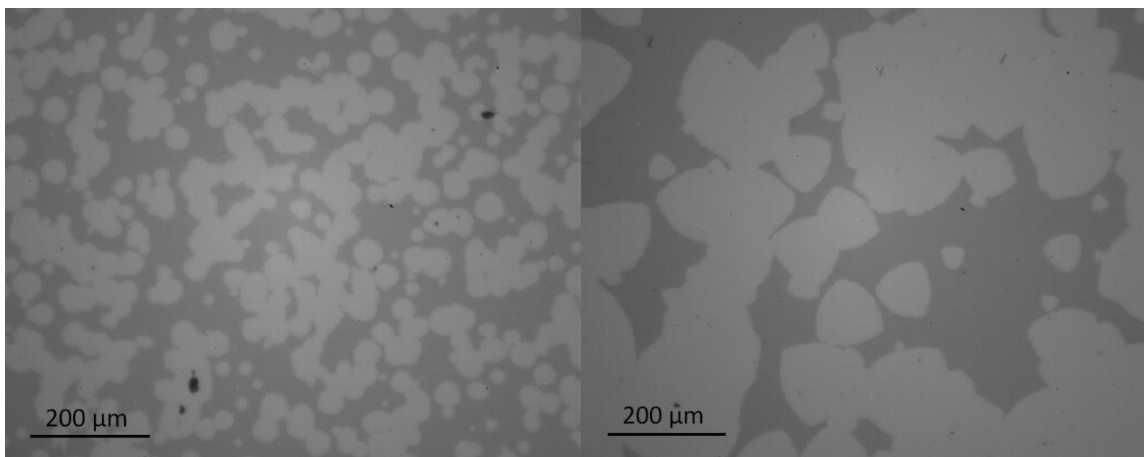


Figure 15. Both images show a partially crystallised sample of 200 nm thick $\text{Ge}_{10}\text{Sb}_{90}$ on glass. On the left is an image of a sample that is heated at 180°C and on the right is an image of a sample that is heated at 188°C . The left image shows only slow growing crystals and the right image shows only fast growing crystals.

4.2 Laser

First, some measurements were done with setup 3 (see section 3.2.3 and Figure 11). The results are presented in section 4.2.1. During the measurements there was a problem with the readout of the current; the intensity kept rising. It was still possible to find the maximum value and, therefore, to focus the sample, but it was not possible to measure the change in intensity. Therefore, when the beam splitter was delivered earlier than expected, it was decided to yet build setup 2 (see section 3.2.2 and Figure 8 and 10) and see if this solved the problem. The results of the measurements done with this setup are described in section 4.2.2.

4.2.1 Setup 3

First a series of measurements was done with a laser power of 100 mW while the sample of $\text{Ge}_{10}\text{Sb}_{90}$ was in focus. The pulse duration was exponentially varied between 100 μs and 1 ns. Because nothing was acquired, the pulse duration was lengthened from 200 μs to 1 s. Now, as shown in Figure 16, crystallised spots were obtained over the total range of pulse durations. The smallest crystal had a size of about 8 by 17 μm .

In the crystals corresponding to pulse durations of 1 s, 500 ms, 200 ms and 100 ms the crystal was ablated in the middle, which means that either the power was too high or the pulse duration was too long. The crystals corresponding to pulse durations from 50 ms to 200 μs were not burnt in the middle and became smaller as the pulse duration became larger.

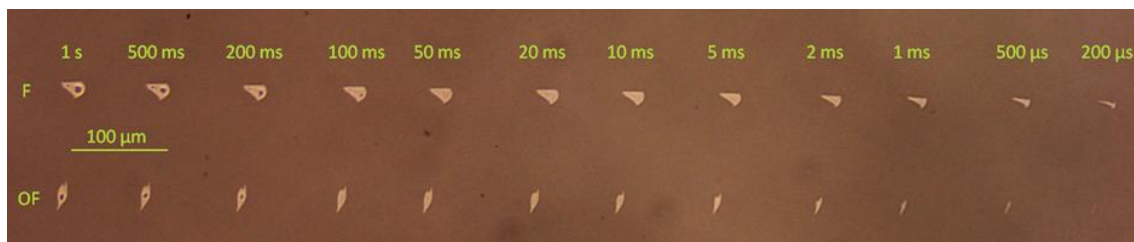


Figure 16. Crystal spots in 200 nm thick $\text{Ge}_{10}\text{Sb}_{90}$ made with 100 mW laser pulses using setup 3. The crystals in the top row were made while the sample was focussed, the crystals in the bottom row were made while the sample was unfocussed. Above the crystal spots the pulse durations are given.

Secondly, a series of measurements were done once more with a laser power of 100 mW, but this time the sample was out of focus. The pulse duration was again exponentially varied from 1 s to 200 μs . Again crystals were obtained for every pulse duration, but this time they were smaller, as shown in Figure 16, and had a different form. Only the crystals corresponding to pulse durations of 1 s, 500 ms and 200 ms were burnt in the middle, the others were not.

4.2.2 Setup 2

As said before, when the beam splitter was delivered, setup 2 was built. The first experiment done was again to investigate the crystal growth in $\text{Ge}_{10}\text{Sb}_{90}$ films when irradiated with a high power laser with a power of 100 mW while the sample was in focus. This time a series of twenty exponentially distributed pulses with a duration between 1 s and 500 ns was performed. As shown in Figure 17, crystals appeared at a pulse duration from 1 s to 5 μs . For a pulse duration of 2 μs or shorter no crystals were visible. The smallest crystal, grown with a pulse duration of 5 μs , had a size of approximately 1 by 6 μm .

With setup 3, no crystals grew with a pulse duration of 100 μs or shorter. Setup 2 thus shows a better crystal growth, which is probably because of a better alignment. With setup 2, the crystals grown at a pulse duration up to 1 ms were damaged in the middle. With setup 3 only pulse durations down to 100 ms showed this damage. This agrees with setup 2 being better aligned.

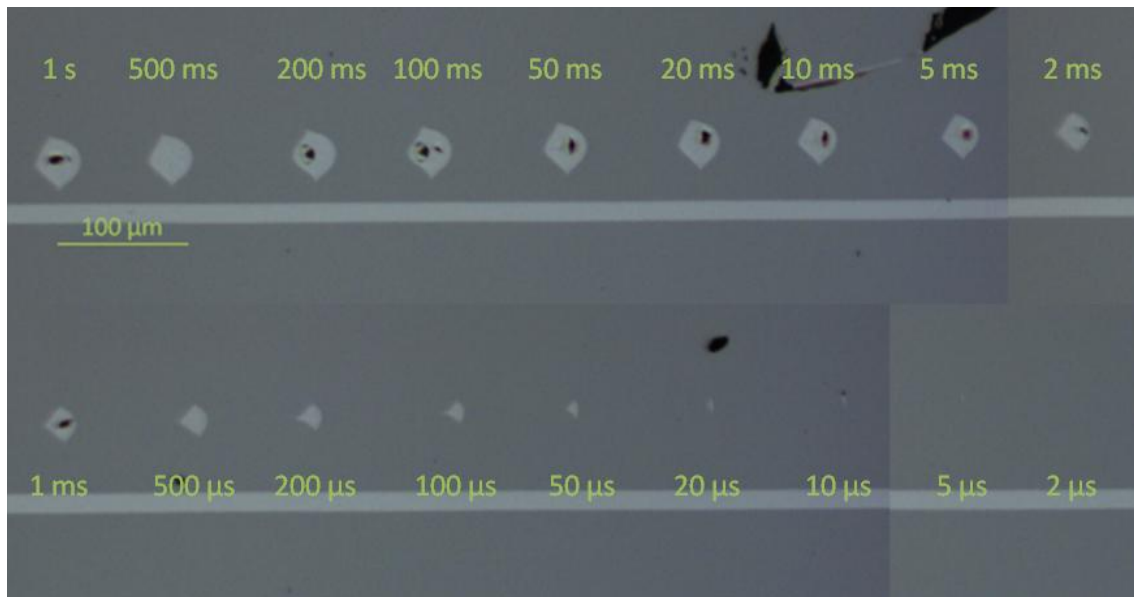


Figure 17. Crystal spots in 200 nm thick $\text{Ge}_{10}\text{Sb}_{90}$ made with 100 mW laser pulses using setup 2. The crystals were made while the sample was focussed. Above (top row) and under (bottom row) the crystal spots the pulse durations are given.

The crystal spots in the previous measurements were not circular, but looked more like a wedge of pie. Figure 18 shows a close up of the crystal that arose after 50 μs of irradiation with a power of 100 mW using setup 2. This crystal looks like a wedge of pie. At first it was thought that this might be because of coma, since, as described in section 2.4, the coma image of a point source also looks like a pie slice. However, it does not seem logical that this image is due to coma, because then it is expected that the burnt part in the crystal is at the vertex of the cone. In contrast, as can be seen in Figure 16, the crystals were ablated at the base.

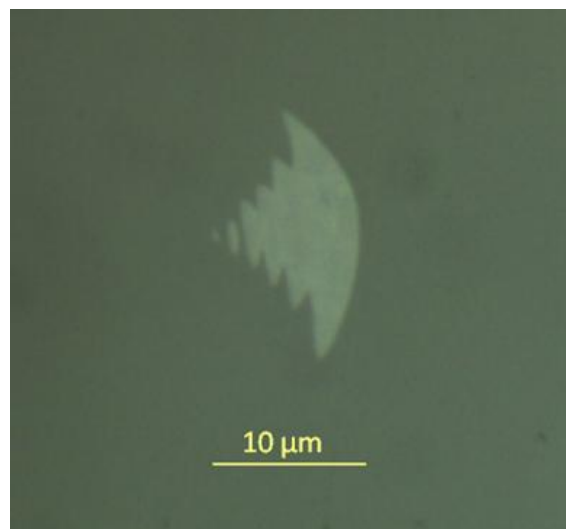


Figure 18. Close up of the crystal in 200 nm thick $\text{Ge}_{10}\text{Sb}_{90}$ that grew after 50 μs of irradiation with a 100 mW laser pulse using setup 2. It shows a comet like crystal.

There are two possible reasons for the crystals not being round. The first is that there was a small scratch on the lens and the second is that the setup was not very stable. A new lens was ordered and placed to resolve the problem with the scratch. To stabilise the setup, the turning mirror was placed nearer to the dichroic beam splitter using shorter connecting rods. After these improvements new measurements were done.

With the improved setup 2, the crystal growth in $\text{Ge}_{10}\text{Sb}_{90}$ films was once more investigated after irradiation with a laser with a power of 100 mW while the sample was in focus. This time the pulse durations were exponentially divided between 1 ms and 100 ns. As can be seen in Figure 19, this time the spots were perfectly round, so either the better stability or the new lens had helped to solve the problem of strangely shaped crystals. The crystals were visible from 1 ms down to 500 ns and were burnt in the middle down to 10 μs . The smallest crystal, grown at 500 ns, had a size of only about 3,4 μm .



Figure 19. Crystal spots in 200 nm thick $\text{Ge}_{10}\text{Sb}_{90}$ made with 100 mW laser pulses using the improved setup 2. The crystals were made while the sample was focussed. Above the crystal spots the pulse durations are given. The crystals are almost perfectly round.

5 Discussion

5.1 Heating Plate

In the samples that were preheated the crystals grew significantly faster than in the samples that were not. This phenomenon can be explained on the basis of the structural relaxation in amorphous materials. In this research the samples that were used had an as-deposited amorphous structure, which is a structure that is far from equilibrium. When the $\text{Ge}_7\text{Sb}_{93}$ films were preheated, the as-deposited amorphous structure relaxed towards an amorphous structure that has a lower Gibbs free energy. This process is called structural relaxation. The lower energy structure is more compatible with the crystalline structure and therefore the crystal growth could proceed more easily and thus faster in the preheated samples.

Two measurements that were done with the $\text{Ge}_7\text{Sb}_{93}$ films were not included in the determination of the trend lines of Figure 13, which will be discussed below.

The red square in Figure 13 is located on the line of the results of the samples that were directly heated to the desired temperature, although this data point corresponded to the sample that was preheated at 100 degrees. In this sample the crystals were still not observed with the high-speed camera after four hours of heating while in the other experiments at this temperature the crystals were observed after about half an hour. This is because there were much less nuclei per unit area. The crystals that have grown in this sample were in four hours as big as crystals in other samples in two and a half hours. For these reasons this result was not included in the determination of the trend line. Why the results of this sample were this dissimilar from the other samples is not clear. Possibly something happened with this sample or perhaps it was of a slightly different composition than the other samples. For a next research it could be interesting to explore if the amount of crystals per area is different for the preheated and not preheated groups.

To slightly accelerate the experiments, at a certain point four samples were simultaneously heated at 100 °C for 12 hours. After these 12 hours in three of the four samples there were no crystals, but in one there were. This sample with crystals contained some scratches that may have increased the facilitated nucleation of crystals. The growth rate of these crystals was examined and the result is shown in Figure 13 as a red circle. This red circle is near the trend line, but determining this growth rate was not very accurate because the high-speed camera was maximally zoomed out and therefore the crystals were very small. That is why this result was not included in the determination of the trend line either.

In the experiment with films of $\text{Ge}_9\text{Sb}_{91}$, the series of images of the first sample at 180 °C were not in focus. Only some small crystals with a radius of approximately 17 pixels had grown yet once the heater was turned off. The sample was placed in a box for a day and the next day it was heated to 180 °C again. When the heater was around 178 °C something unexpected happened; the crystals of the fast type started to grow out of the already existing crystals and filled the screen within one minute. It might be very interesting to further investigate this behaviour.

5.2 Laser

Two problems for the measurements with the laser remain. The first is that there seems to be a problem with focusing the laser onto the sample. Figure 20 shows the results of a test with the focusing, where the sample was either: unfocused 20 and 40 μm anticlockwise, focussed or unfocused 20 and 40 μm clockwise. Here the pulse duration was logarithmically varied from 1 s to 100 μs . The crystals where the sample was focussed and where the sample was 40 μm clockwise unfocussed were very similar. The crystals of the sample being 20 μm clockwise unfocussed were smaller than the rest and had a larger ablated part. Therefore this sample seemed to be more focussed than the sample that was originally thought to be focussed. Apparently, when the low power laser is in focus it does not mean that the high power laser is also focussed. For a next research it would be interesting to test this focusing from focus to 40 μm clockwise unfocussed in steps of 5 μm to see if it is possible to optimise the focusing.

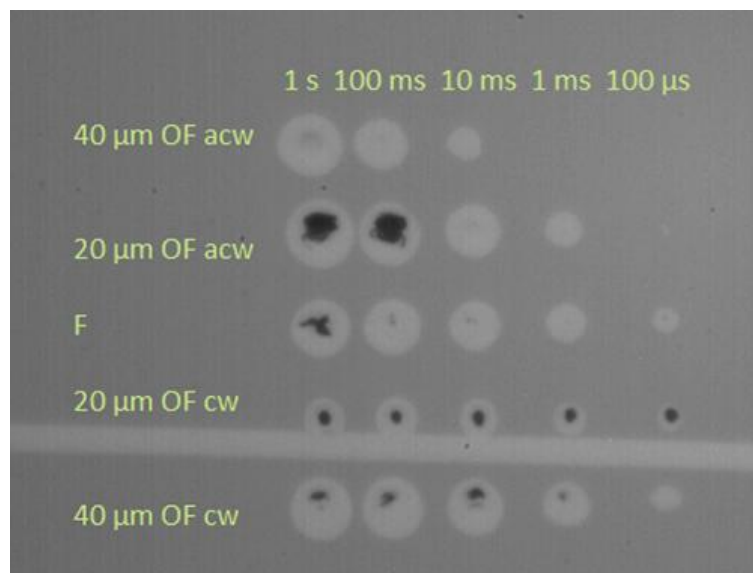


Figure 20. This shows the results of a test of focusing the sample. The crystals that grew while the sample was in focus and while the sample was 40 μm out of focus seem to be very similar. It looks like the sample was best focussed when it was thought to be 20 μm out of focus.

The second problem that remains is that it is not possible to investigate the crystals by intensity. It was planned, and programmed in the script of G. Eising, that the crystal growth can be measured based on the change of the intensity of the reflected beam. During the experiments with setup 2 it became clear that the intensity did not change after irradiation. It could be that the crystals grown were too small to change the intensity noticeably. In the future this could be tested with a sample of another composition, where the crystals grow faster and therefore larger, or using the same composition with a longer pulse duration at a lower power, so the crystals have more time to become large but not burnt.

Finally, for a future study it would be good to see if it is possible to grow larger crystals that are not ablated in the middle. These crystals can be used to investigate the possibilities of melt-quenching, and thereafter again crystallising, the samples with the high power laser.

6 Conclusions

During this bachelor research it became clear that when a sample of $\text{Ge}_7\text{Sb}_{93}$ is preheated at $100\text{ }^\circ\text{C}$ for 12 hours and thereafter heated to the final temperature, the crystals grow about 50 per cent faster than the crystals that grow in a sample that is immediately heated to the final temperature. This is because after preheating, the as-deposited amorphous structure relaxes such that it becomes more compatible with the crystalline structure. Therefore, the crystal growth could proceed more easily and thus faster in the preheated samples. In $\text{Ge}_{10}\text{Sb}_{90}$ films this effect is probably also present, but this was not measurable, because the analysing software was not accurate enough.

In a sample of $\text{Ge}_9\text{Sb}_{91}$ only slow crystals grow at a temperature of $180\text{ }^\circ\text{C}$ and only fast crystals grow at a temperature of $188\text{ }^\circ\text{C}$. In between these temperatures, both crystals grow in the sample, but the closer to $180\text{ }^\circ\text{C}$ the more slow growing crystals are present and the closer to $188\text{ }^\circ\text{C}$ the more fast growing crystals are present. It would be interesting to further investigate the behaviour if the sample is first heated to $180\text{ }^\circ\text{C}$ for a short time so only small crystals have grown, thereafter cooled down to room temperature and again heated to $180\text{ }^\circ\text{C}$, because in this research it was discovered by accident that in this case the fast crystals were already formed at $178\text{ }^\circ\text{C}$.

It became apparent that it is possible to build a setup whereby crystals grow in a sample of $\text{Ge}_{10}\text{Sb}_{90}$ after irradiation with a high power laser. Nevertheless, much remains to be improved to the setup that is conceived and built the last 10 weeks. The focusing that was obtained by using a low power laser is still not precise enough to get reliable results and it is not yet possible to get information about crystal growth by analysing the intensity of the reflected low power laser beam. A next research should give a better idea of the possibilities of crystallisation and melt-quenching using a high power laser.

7 Special Thanks

At first I would like to thank Bart Kooi for being my first supervisor and giving me the opportunity to do my bachelor research at this group.

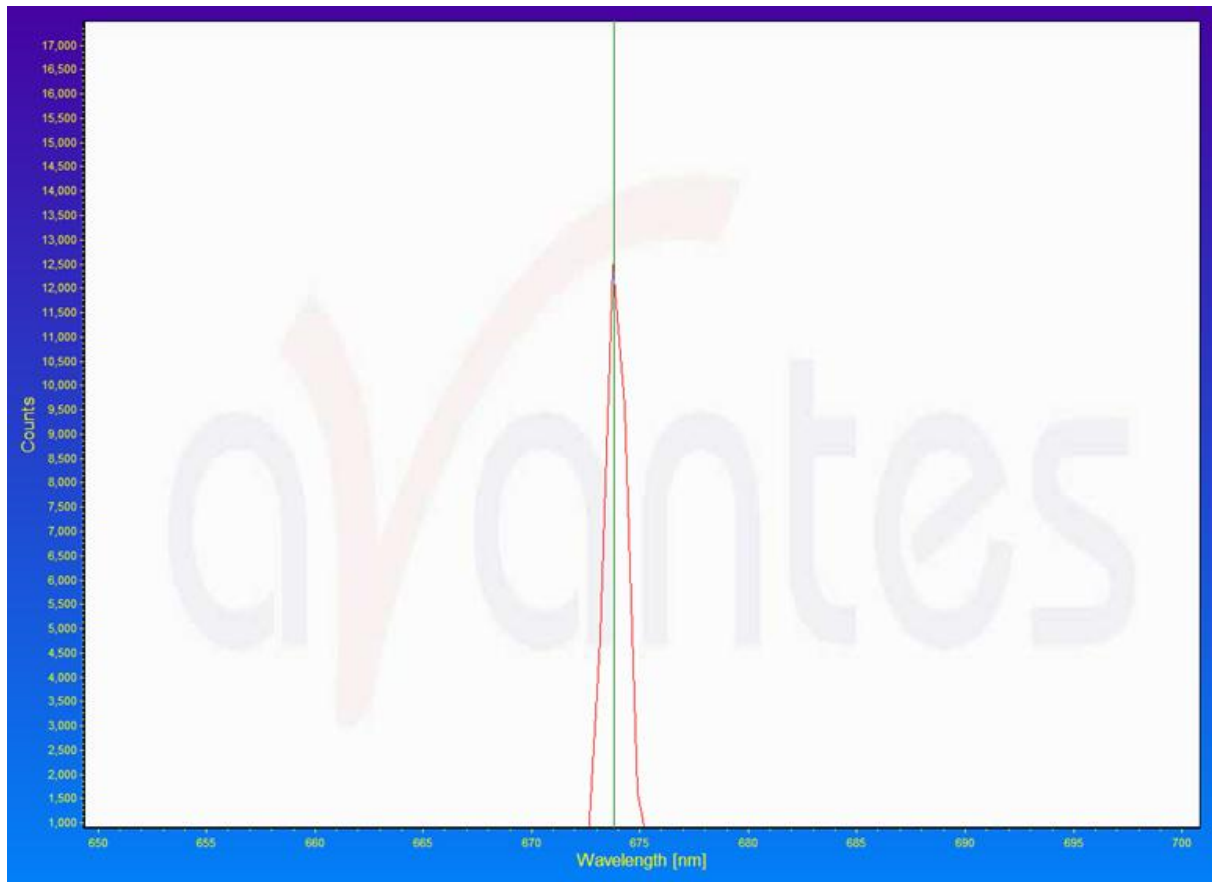
As well, I would like to thank Gert Eising for being my daily supervisor. If I had problems, I could go to him and we tried to solve them together. He also helped me greatly with designing the setup for the laser experiment and deciding which components needed to be ordered.

To finish, many thanks to the whole NMI-group for all the delicacies and for being such a good company these 10 weeks.

8 References

- [1] Raoux, S. & Wuttig, M. (2009). *Phase Change Materials: Science and Applications*. New York: Springer.
- [2] Krusin-Elbaum, L., Shakhvorostov, D., Cabral Jr., C., Raoux, S. and Jordan-Sweet, J.L. (2010). Irreversible altering of crystalline phase of phase-change Ge-Sb thin films. *Applied Physics Letters*, 96, 121906. doi: 10.1063/1.3361656
- [3] Callister, W.D. & Rethwisch, D.G. (2011). *Materials Science and Engineering*. Hoboken, NJ: John Wiley & Sons.
- [4] Retrieved from <http://muhendishane.org/kutuphane/temel-malzeme-bilgisi/amorfyapida-keramikler>
- [5] Gholipour, B., Hewak, D.W., Huang, C.C., Al-Saab, F., Anastasopoulos, A., Guerin, S., Hayden, B. & Purdy, G. (2011). Investigation of the scalability limit and thermal stability of low current consuming, nanowire phase change memory cells for high density commercial applications. [Summary of a speech on E\PCOS 2011]. Retrieved from http://www.epcos.org/library/papers/pdf_2011/Posters-Contributed/PC-14.pdf
- [6] Kokorowski, S.A., Olson, G.L. and Hess, L.D. (1982). Kinetics of laserinduced solid phase epitaxy in amorphous silicon films. *Journal of Applied Physics*, 53, 921. doi: 10.1063/1.330561
- [7] Arrhenius equation. (2013). *Wikipedia, the free encyclopedia*. Retrieved Januari 22, 2013, from http://en.wikipedia.org/wiki/Arrhenius_equation
- [8] Siegel, J., Afonso, C.N. and J. Solis. (1999). Dynamics of ultrafast reversible phase transitions in GeSb films triggered by picosecond laser pulses. *Applied Physics Letters*, 75, 3102. doi: 10.1063/1.125244
- [9] Solis, J., Afonso, C.N., Hyde, S.C.W., Barry, N.P. and French, P.M.W. (1996). Existence of Electric Excitation Enhanced Crystallization in GeSb Amorphous Thin Films upon Ultrashort Laser Pulse Irradiation. *Physical Review Letters*, 76, 2519.
- [10] Keller, H.E., Spring, K.R., Long, J.C. and Davidson, M.W. (2012). Comatic Aberrations. Retrieved from <http://www.olympusmicro.com/primer/java/aberrations/coma/index.html>
- [11] Types of Aberrations. Retrieved from http://www.thorlabs.com/newgrouppage9.cfm?objectgroup_id=3208
- [12] Retrieved from http://www.thorlabs.com/newgrouppage9.cfm?objectgroup_id=3313

Appendix A



The wavelength of the low power laser was measured with a spectrometer. As shown in the image above it measured a wavelength of about 674 nm

Appendix B

This is the Matlab script for the analysis of the intensity of the reflection:

```
function intensitygraph = matrixanalysis (testmatrix);
matrix = importdata(testmatrix);
data = matrix.data;
measurement = data(:,1);
xvalue = data(:,2);
yvalue = data(:,3);
pulsetime = data(:,4);
power = data(:,5);
intensity_before = data(:,6);
intensity_after = data(:,7);
intensity = intensity_after - intensity_before;
xaxis = unique(power);
yaxis = unique(pulsetime);
output = zeros(length(xaxis),length(yaxis));

for i = 1:length(intensity);
    xindex = find(xaxis == power(i));
    yindex = find(yaxis == pulsetime(i));
    output(xindex,yindex) = intensity(i);
end

pcolor(yaxis,xaxis,output);
```